







ORIGINAL RESEARCH

Impact of individual, combined and sequential stress on photosynthesis machinery in rice (*Oryza sativa* L)

Khalid Anwar¹ | Rohit Joshi¹  | Rajeev N. Bahuguna^{1,2}  | Govindjee Govindjee³  |
Rashmi Sasidharan⁴  | Sneh L. Singla-Pareek⁵  | Ashwani Pareek^{1,2} 

¹Stress Physiology and Molecular Biology Laboratory, School of Life Sciences, Jawaharlal Nehru University, New Delhi, India

²National Agri-Food Biotechnology Institute, Mohali, Punjab, India

³Department of Biochemistry, Center of Biophysics & Quantitative Biology, and Department of Plant Biology, University of Illinois at Urbana-Champaign, Urbana, IL, USA

⁴Plant Stress Resilience, Institute of Environmental Biology, Utrecht University, The Netherlands

⁵Plant Stress Biology, International Centre for Genetic Engineering and Biotechnology, Aruna Asaf Ali Road, New Delhi, India

Correspondence

Ashwani Pareek,
Email: ashwanip@mail.jnu.ac.in

Present address

Rohit Joshi, Division of Biotechnology, CSIR-Institute of Himalayan Bioresource Technology, Palampur, Himachal Pradesh, India.

Funding information

Department of Biotechnology, Ministry of Science and Technology, India, Grant/Award Number: BT/IN/NWO/15/AP/2015-16

Edited by V. Hurry

Abstract

Abiotic stresses such as heat, drought and submergence are major threats to global food security. Despite simultaneous or sequential occurrence of these stresses being recurrent under field conditions, crop response to such stress combinations is poorly understood. Rice is a staple food crop for the majority of human beings. Exploitation of existing genetic diversity in rice for combined and/or sequential stress is a useful approach for developing climate-resilient cultivars. We phenotyped ~400 rice accessions under high temperature, drought, or submergence and their combinations. A cumulative performance index revealed *Lomello* as the best performer across stress and stress combinations at the seedling stage. *Lomello* showed a remarkable ability to maintain a higher quantum yield of photosystem (PS) II photochemistry. Moreover, the structural integrity of the photosystems, electron flow through both PSI and PSII and the ability to protect photosystems against photoinhibition were identified as the key traits of *Lomello* across the stress environments. A higher membrane stability and an increased amount of leaf chlorophyll under stress may be due to an efficient management of reactive oxygen species (ROS) at the cellular level. Further, an efficient electron flow through the photosystems and, thus, a higher photosynthetic rate in *Lomello* is expected to act as a sink for ROS by reducing the rate of electron transport to the high amount of molecular oxygen present in the chloroplast. However, further studies are needed to identify the molecular mechanism(s) involved in the stability of photosynthetic machinery and stress management in *Lomello* during stress conditions.

1 | INTRODUCTION

The global human population is expected to reach 9.7 billion by 2050, which requires that the production of major cereal crops be increased by 70–100% to help meet the global food demand (Tilman et al., 2011). A significant improvement in wheat and rice production has been achieved during and after the green revolution through the development of high-yielding semi-dwarf varieties, chemical inputs, and technological advancement in crop cultivation practices (Eliazer-Nelson et al., 2019). However, the rate of gain in productivity has slowed down substantially in recent decades, and

the productivity of rice and wheat has already reached a plateau (Grassini et al., 2013). On the other hand, limiting resources of fresh water and land, and increased frequency and severity of extreme weather events due to climate change are posing a serious threat to global food security. Recent evidence has shown that the impact of heat spikes, drought spells and floods at the regional scale has resulted in heavy yield penalties leading to complete crop failures at sensitive growth stages (Schauberger et al., 2017; Yeung et al., 2018). Therefore, development of climate-resilient crops is a major goal to sustain higher productivity in the current and future environment.

The majority of crop improvement studies in the past have focused on understanding the response of crops to selected individual stresses, providing insights into crop responses under single stress (Kadam et al., 2017; Joshi et al., 2018, 2020; Bahuguna et al., 2022). However, crop plants seldom face single stress, particularly under natural field conditions, where multiple stresses occur simultaneously or sequentially during the crop cycle (Suzuki et al., 2014; Anwar et al., 2021). Interestingly, a combination of two or more stresses is not merely the sum of individual stresses but is considered a new state of stress (Coolen et al., 2016; Yadav et al., 2022). Therefore, plant response to stress combinations is unique and warrants systematic investigation to understand the mechanistic basis of plant adaptation under abiotic stress combinations. Despite the substantial advances made thus far towards the understanding of the impact of individual stresses, plant responses to the combination of stresses, occurring dynamically at temporal and spatial scales in the environment, are largely unknown.

Photosynthesis is a fundamental physiological process in plants (Ort et al., 2022). Therefore, a better understanding of how plants modulate light harvesting and use it to enhance photosynthesis efficiency is necessary to maintain crop yield under both optimum and suboptimal environments (Kromdijk et al., 2016). It is already known that the occurrence of different abiotic stresses, such as heat, drought, salinity, and submergence, during different crop growth phases negatively affect the rate of crop growth and productivity mainly by changing the photosynthesis process by (1) reducing the rate of electron transport (Foyer et al., 2012), (2) increasing photooxidative stress in different organs (Munoz & Munné-Bosch, 2017), (3) inactivating the key enzymes *Rubisco* and *Rubisco activase* (Yamori and von-Caemmerer, 2009), (4) decreasing the photosynthesis pigment-protein complexes (Rantala et al., 2020), and (5) enhancing the production of the reactive oxygen species (ROS) (Choudhury et al., 2017). We emphasize that PSII is one of the most susceptible components of the photosynthesis machinery, and its performance, measured through chlorophyll (Chl) *a* fluorescence, is highly sensitive to environmental stresses (Stirbet et al., 2018). Moreover, the increased intracellular concentration of ROS hampers the repair mechanism of PSII, making it more sensitive to photodamage (Nishiyama & Murata, 2014). Therefore, Chl *a* fluorescence is considered the most powerful tool to quantify the impact of stress on the photosynthesis process. Further, different parameters related to Chl *a* fluorescence have been established to detect PSII photochemical efficiency and to estimate the impact of different stresses on photosynthesis machinery. Crop plants show wide genetic variability for photosynthesis (Bahuguna et al., 2022). Interestingly, the ability of a genotype to maintain photosynthesis, particularly under any stressful environment, depends upon multiple factors such as robust antioxidative defence machinery, higher accumulation of photosynthesis pigments, better photosystem stability, and altered composition of thylakoid membranes (Kobayashi et al., 2016). Hence, stable photosynthesis machinery under a sub-optimal environment is a crucial marker for stress tolerance (Bahuguna et al., 2022).

Rice is the most important cereal crop and staple food for the majority of the world population living in Asia and Africa. The sensitivity of rice to

major abiotic stress such as heat (Jagadish et al., 2010), drought (Kadam et al., 2017), and flooding (Bailey-Serres et al., 2012) is well documented. However, under natural conditions, heat and drought are considered the most obvious stress combinations which occur simultaneously, mostly in semi-arid or drought-stricken areas, affecting the physiology and metabolism of rice and resulting in a substantial reduction in the yield as well as in grain quality. On the other hand, low-land rain-fed rice is extremely vulnerable to partial or complete submergence (Bailey-Serres et al., 2010). Restricted gas diffusion underwater, coupled with the often-reduced light availability in flood waters, can lead to tissue hypoxia. Once the floodwaters recede, re-exposure to high light and high oxygen conditions can lead to oxidative stress, dehydration and rapid deterioration of plant growth (Yeung et al., 2018). Thus, flooding is generally considered a sequential stress where the post-submergence period exposes plants to a second set of stressors. Genetic improvement in elite rice cultivars for individual stress is often ineffective under stress combinations due to distinct defence mechanisms functional under each stress condition (Suzuki et al., 2014; Yadav et al., 2022). Considering that exposure to multiple stresses is inevitable in field crops, particularly in the current and more so in the future environment, it is a prerequisite to understand how plants regulate and prioritize their adaptive response(s) when exposed to different stresses individually, sequentially or simultaneously.

Natural genetic variation among species provides an inherent capacity for ecological adaptation and acclimation (Loudet & Hasegawa, 2017). Rice has substantial genetic diversity due to its adaptation under extremely variable environments (De Kort et al., 2021). Nevertheless, only a fraction of this information has been utilized in identifying the potential donor genotypes, novel quantitative trait loci (QTLs), and novel genes (Patra et al., 2016). Indeed, exploring genetic diversity is expected to help in understanding the phenotypic plasticity and mechanistic basis of rice acclimation and adaptation under complex stress environments (Zhang et al., 2017; Bahuguna et al., 2022). Hence, we phenotyped ~400 globally collected rice accessions to characterize their responses to heat and drought as co-occurring combinations and post-submergence drought as sequential abiotic stress. The major objectives were to (1) identify the potential donor genotype for individual, combined and sequential abiotic stress tolerance and (2) characterize a contrasting set of rice genotypes to delineate the impact of individual and combination stresses on photosynthesis and Chl *a* fluorescence kinetics. This study demonstrated that photosystem stability, electron transfer, and efficiency of alternate electron acceptors, along with robust defence from oxidative stress, could allow *Lomello* to maintain an equilibrium of photosynthetic electron transport and the efficiency of photosystems across stress conditions.

2 | MATERIALS AND METHODS

2.1 | Choosing rice accessions

A diverse panel of 394 rice (*Oryza sativa*) accessions (Anwar et al., 2022) was used for this study, consisting of 75 indica, 53 aus,

16 aromatic, 100 temperate japonica, 86 tropical japonica, and 64 admixed genotypes (Table S1). This panel was originally assembled at the International Rice Research Institute, Philippines (<https://www.irri.org/international-rice-genebank>). The study was conducted under controlled plant growth chambers with the inner dimensions of 1200 × 600 × 1200 cm (Labtech India Pvt. Ltd.). Two independent experiments were conducted during 2018 and 2019. In Experiment I, 394 rice genotypes were phenotyped under individual (heat, drought, submergence), combined (heat + drought) and sequential (submergence followed by drought) stress to identify a contrasting set (the best and least performing) of genotypes at the early vegetative stage. In Experiment II, a more detailed characterization of the selected contrasting set of genotypes was carried out on the basis of their Chl *a* fluorescence kinetics under similar stress combinations used in Experiment I. These detailed investigations were carried out at four stages, i.e., mild, moderate and severe stages of stress, followed by the recovery phase.

2.2 | Phenotyping of the rice genotypes (Experiment I)

In 2018, seeds of 394 rice genotypes were surface sterilized and allowed to germinate in the dark at 28/23°C (day/night) and at 65–70% relative humidity for 2–3 days (Lakra et al., 2018). Germinated seeds were then sown into thermocol (polystyrene) pots of 8 cm diameter and 12 cm height containing 2 mm sieved soil mixed with 320 mg Kg⁻¹ ammonium sulphate (nitrogen source), 170 mg Kg⁻¹ single super phosphate (phosphorous source) and 170 mg Kg⁻¹ muriate of potash (potassium source) with a final weight of each pot maintained at 180 g before sowing. Four healthy seedlings were maintained in each pot, and 30 pots per genotype were used for the study, thus making a total of 11820 pots. Adequate moisture level was maintained in pots to keep the soil at fully saturated condition. All the pots were kept under 12/12 h light/ dark period at 28/ 23°C ± (SD 2°C) day/ night temperature. Blue-red LED light panels were used in the chambers as a light source to provide ~800 μmol photons m⁻² s⁻¹ photosynthetically active radiation (PAR) measured by PAR sensors (Apogee Instruments) placed within each growth chamber. Optimum growth conditions were maintained across all the growth chambers until 14 days after sowing. After 14 days, individual sets of 1970 pots containing five pots for each genotype were subjected to the following individual treatments: (1) control, by maintaining pots at fully saturated condition, and chamber temperature at 28/23°C (day/night), (2) heat stress (HT), by raising day/night temperature on the 15th day to 35/29°C (day/night) in the dedicated growth chamber for subsequent 7 days, (3) drought (D), by withholding water until the soil water content (SWC) reached ~30–40% of the initial soil water content (~100%), and the pots were maintained at 28/23°C (day/night) temperature, (4) submergence (S), by completely submerging the seedlings for subsequent 7 days in an acrylic tank, (5) combined high temperature and drought stress, by withholding watering until the soil water content reached ~30–40% of the initial soil water content, and

the temperature was maintained at 35/29°C (day/night), (6) post submergence drought stress (PSD), by initially submerging the pots for 7 days followed by withholding watering until soil water content reached ~30–40%; the temperature of the chamber was maintained at 28/23°C (day/night). In all cases, the light conditions and relative humidity were maintained at ~800 μmol photons m⁻² s⁻¹ PAR and 65–70%, respectively, across the treatments except during submergence, when the light intensity of 160 μmol photons m⁻² s⁻¹ was used (Figure S1). Drought stress was monitored by following the gravimetric method as described in detail by Kadam et al. (2015, 2017). Additionally, soil water content was also recorded at different time points during the drought stress period using a soil moisture sensor (Water Scout SM 100, Spectrum Technologies, Inc., Aurora, IL 60504).

2.3 | Measurements of various growth-related parameters

Shoot length, root length, total fresh weight, total dry weight, and root biomass were measured manually using a metric scale and an analytical weighing balance (Sartorius). (For the sampling time and the observation timeline, see Figure S1). Dry weight was measured for seedlings that were oven-dried at 65°C for 72 h. A non-destructive measurement of the greenness index indirectly indicating chlorophyll/nitrogen content of the topmost fully expanded leaf was measured using a SPAD (Soil Plant Analysis Development) 502 chlorophyll meter (Konica Minolta Inc.). Destructive harvesting for measuring electrolyte leakage was done in liquid nitrogen, and the topmost fully expanded leaf samples were kept at –80°C for further analysis. Electrolyte leakage was measured and calculated to assess the extent of membrane damage, as described by Joshi et al. (2018).

2.4 | Clustering and performance ranking analysis

The most and the least tolerant genotypes across all the stress treatments were identified by doing clustering and performance ranking analysis. Performance ranking was based on (1) phenotypic plasticity (relative performance of a genotype in the treatment with respect to the control) and (2) absolute performance of a genotype within the treatment. Data obtained for different traits was normalized since different traits were measured in different scales and units. The normalization step considered the mean and the variance of the trait within the population, such that the units are deleted, and all traits were measured on an equivalent scale:

$$X_{i,d}^n = \frac{X_{i,d} - \mu_{X,d}}{\sigma_{X,d}}$$

where, 'i' is a genotype, 'n' normalized value of trait, $\mu_{X,d}$ and $\sigma_{X,d}$ are the mean and standard deviation of the trait *X* under treatment *d* for the entire population.

The sum of the normalized traits for each genotype was used for determining the performance of the genotype i under the treatment d , which was calculated as:

$$P_{i,d} = FW_{i,d}^n + DW_{i,d}^n + SPAD_{i,d}^n + RL_{i,d}^n + SL_{i,d}^n + RB_{i,d}^n - EL_{i,d}^n,$$

where, the normalized traits are total plant fresh weight ($FW_{i,d}^n$), total plant dry weight ($DW_{i,d}^n$), SPAD value ($SPAD_{i,d}^n$), root length ($RL_{i,d}^n$), shoot length ($SL_{i,d}^n$), root biomass ($RB_{i,d}^n$), and electrolyte leakage ($EL_{i,d}^n$). Higher electrolyte leakage indicates lower performance, hence, given a negative value in the above formula.

2.5 | Detailed characterization of the selected contrasting set of genotypes (Experiment II)

In 2019, a contrasting pair of genotypes, *Lomello* (tolerant) and C57-5043 (sensitive), selected based on the screening in Experiment I, were taken for comparison and for further characterization along with known tolerant check N22 (for heat, drought), and elite cultivar IR64. Pots, soil, nutrients, temperature, humidity, and light conditions were kept similar to those described under Experiment I. A detailed characterization of these genotypes was done on the basis of Chl *a* fluorescence kinetics. The stress exposure period was divided into three parts (mild, moderate, and severe) based on stress level and duration in order to understand the acclimation responses (i.e., adaptation) under combined and sequential stresses. A period of

three hours was used for sampling in the recovery phase after the end of stress exposure (Figure 1). Non-destructive phenotyping, such as SPAD, and gas exchange traits were measured from the fully developed top leaf. To minimize the influence of circadian rhythm on the observations, all the data were collected at the same time (11:00 h) throughout the stress period (McClung, 2006).

Sampling and observations were taken at four-time points, i.e., under mild stress, moderate stress, severe stress, and recovery. For the high temperature (35/29°C) condition, sampling was done on the 3rd day (mild), the 5th day (moderate), and the 7th day (severe) of stress. For the drought stress observations, samplings were done when soil water content (SWC) reached ~80% (mild), ~60% (moderate), and ~40% (severe). For the samples under submergence stress, observations were made on the 4th day (mild), the 7th day (moderate), and the 10th day (severe) using an acrylic tank kept at 28/23°C (day/night) temperature and 160 $\mu\text{mol photons m}^{-2} \text{s}^{-1}$ of light. For the combined high temperature + drought stress, the sampling and the observations were made when SWC reached ~80% (mild), 60% (moderate), and 40% (severe) while the temperature of the chamber was kept constant at 35/29°C (day/night). For the sequential stress (post submergence drought), pots were completely submerged for 7 days in acrylic tanks, kept at 28/23°C (day/night) temperature, under a light intensity of 160 $\mu\text{mol photons m}^{-2} \text{s}^{-1}$, followed by withholding watering until SWC reached 80% (mild), 60% (moderate), and 40% (severe). Observations and sampling were also done in the recovery phase, which was 3 h after the termination of each stress exposure, across the treatments. Corresponding observations and samplings

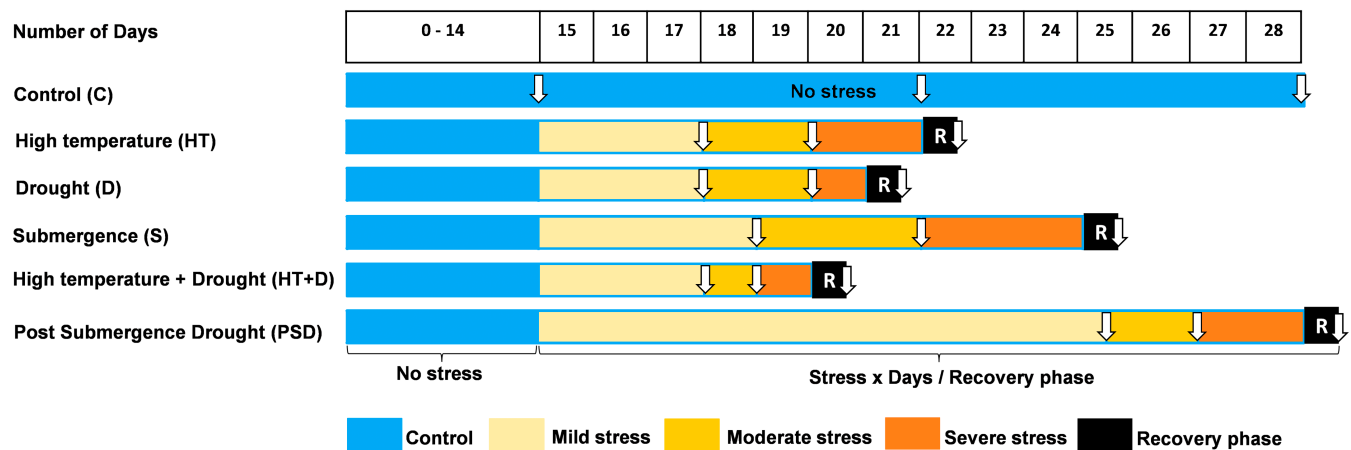


FIGURE 1 Experimental design for assessing the performance of rice genotypes under individual, combined, and sequential stress. The control/well-watered (C) plants were grown at 28/23°C (day/night) with 65–70% relative humidity and without any stress treatment. Observations and sampling were done across the treatments at three time points indicated by white downward arrows. Corresponding samples for the control were taken at 14, 21, and 28 days, respectively. Three different levels of stress are depicted as mild, moderate, and severe stress, and for 3 hours of recovery (R). (1) High temperature [HT; 35/29°C (day/night) for 3 (mild), 5 (moderate), and 7 (severe) days]; (2) Drought [D; withheld watering till soil water content (SWC) reached 80% (mild), 60% (moderate), and 40% (severe) at 28/23°C (day/night) temperature]; (3) Submergence [S; completely submerged for 4 (mild), 7 (moderate), and 10 (severe) days in an acrylic tank at 28/23°C (day/night) temperature, under light intensity of 160 $\mu\text{mol photons m}^{-2} \text{s}^{-1}$]; (4) Combined high temperature + drought stress [HT + D; 35/29°C (day/night) temperature, till soil water content (SWC) reached 80% (mild), 60% (moderate), and 40% (severe)]; and (5) Sequential stress; post submergence drought [PSD; completely submerged for 7 days in an acrylic tank at 28/23°C (day/night) temperature under light intensity of 160 $\mu\text{mol photons m}^{-2} \text{s}^{-1}$, and then watering was withheld till the soil water content (SWC) reached 80% (mild), 60% (moderate), and 40% (severe) at 28/23°C (day/night) temperature].

were taken from the pots kept under control conditions for both genotypes (Figure 1).

2.6 | Measurements of various growth traits

Shoot length, root length, total fresh weight, and total dry weight were measured manually using a metric scale and analytical weighing balance (Sartorius, Argentina). Dry weight was measured after oven drying the samples at 65°C for 72 h.

2.7 | Gas exchange measurements

All the gas exchange measurements, including net photosynthesis rate, stomatal conductance, transpiration rate, and the concentration of internal carbon dioxide, were obtained from the top-most fully expanded leaf, using a portable photosynthesis instrument LI-6400XT (LI-COR Inc.) between 0830 to 1130 h. Before measurements, the CO₂ concentration of the plant sample chamber was adjusted to 400 μmol mol⁻¹ using a [CO₂] mixer provided by the LI-COR CO₂ injection system. A flow rate of 400 μmol CO₂ s⁻¹ and a near-saturating photosynthetic photon flux density (PPFD) of 1200 μmol photons m⁻² s⁻¹ from an inbuilt LI-6400XT LED light source was maintained throughout the measurements. Humidity in the sample chamber was kept at ~65%; readings were taken only after the system had reached stability (Bahuguna et al., 2022).

2.8 | Chlorophyll *a* fluorescence measurement

Chl *a* fluorescence transients were measured using the Plant Efficiency Analyzer Handy PEA (Hansatech Instruments), using the middle part of the top-most fully expanded leaves (Stirbet et al., 2018). Further, the original readings, obtained from the Handy PEA, were normalized both at the “O” level, i.e., at minimum fluorescence (Fo) (measured at 0.05 ms, after the sample was dark-adapted for 20 min) and at the “P” level, i.e. maximum fluorescence (Fm), by using the PEA Plus software (version 1.12), and then the data were analysed using a set of parameters obtained from the fluorescence values on the OJIP curve, these being the proxies of the different characteristics of PSII, and of the photosynthesis electron transport (Strasser & Strasser, 1995) (see Table 1).

2.9 | Statistical analysis

Data were statistically treated, following the analysis of a variance method (ANOVA), using SigmaPlot 12.0 software (Systat Software Inc., San Jose, CA, USA) and GenStat 15th Ed. Rothmstad, Germany. SigmaPlot 12.0 software was used for the graphical presentation of the OJIP Chl *a* fluorescence transient curves, whereas the differences between the control and the stress treatments were separated

according to Tukey's Honest Significant Difference (HSD) post-hoc test at 5% level of significance. Genotype selection via clustering and performance ranking was performed using the R statistical software (version 3.6.0).

3 | RESULTS

3.1 | Phenotyping diverse rice germplasm under individual, combined, and sequential stresses (Experiment I)

A significant genotype × treatment ($P < 0.05$ to 0.001) effect was noted for shoot length ($P < 0.05$), root length ($P < 0.001$), fresh weight ($P < 0.001$) and dry weight ($P < 0.001$). Shoot length showed minor reductions under stress, except that a substantial reduction in shoot length was noted under submergence and post-submergence drought (Figure 2A). Conversely, the root length was reduced significantly across stresses. However, the effect of high temperature on root length was maximum, with a 43 to 59% decline as compared to the control across the genotypes. On the contrary, drought stress showed minimum impact on root length (Figure 2B). Root biomass showed a drastic decline under submergence and post-submergence drought, with 50 to 66% and 33 to 50% reduction, respectively, as compared to the controls (Figure 2C). A significant ($P < 0.001$) decline (8 to 68%) in shoot fresh weight was observed across the stress treatments as compared to the control condition, with high temperature showing the lowest impact (Figure 2D). Moreover, dry weight was significantly ($P < 0.001$) reduced across all the stresses, with a maximum decline observed under submergence stress (75 to 89%), followed by post-submergence drought (33 to 83%) and drought (25 to 84%), as compared to their respective controls (Figure 2E). Genetic variation for electrolyte leakage ranged from 12 to 97% across the stress treatments. However, the effect of submergence on electrolyte leakage was highest (up to 98%) followed by post-submergence drought (Figure 2F).

3.2 | Cumulative performance index

A heat map was developed for the relative performance index of 394 genotypes across the stress treatments, which showed a k-means (via Loyd's algorithm) cluster of the relative performance index of the genotypes across the stress treatments (Figures S2, S3). A list of the ten best and the ten least performing genotypes (based on the heat map analysis) is shown in Figure S2. Further, on the basis of cumulative performance index, *Lomello* with a score of 0.52 (under control condition), 1.68 (under high temperature), 0.18 (under drought), 0.86 (under submergence), 0.27 (under high temperature + drought) and 0.88 (under post submergence drought) was picked as the best-performing genotype across all the stress treatments, whereas *C57-5043* with a score of -0.54 (under control), -0.87 (under high temperature), -0.87 (under drought), 0.2 (under submergence), -0.89 (under high temperature + drought) and -0.54

TABLE 1 Definition of technical fluorescence parameters, energy fluxes, and JIP parameters used in this study to analyze O-J-I-P, the chlorophyll *a* fluorescence transient (Strasser et al., 2004; Stirbet and Govindjee, 2011; Tsimilli-Michael, 2019). *Abbreviations:* PSI, PSII, RC, and Q_A are for photosystem I, photosystem II, total number of active PSII reaction centers in the measured area, and the first plastoquinone electron acceptor of PSII, respectively.

Fluorescence parameters	Definitions
t_{Fm}	Time to reach the maximum fluorescence, F_m
$F_0 = F_{0.05ms}$	Minimum (initial) fluorescence
F_m	Maximum fluorescence
$F_J = F_{2ms}; F_I = F_{30ms}$	Fluorescence at the J-step ($t = 2$ ms); and at the I-step (at $t = 30$ ms)
$F_v = F_m - F_0$	Maximum variable (v) fluorescence
$V_J = (F_J - F_0)/F_v; V_I = (F_I - F_0)/F_v$	Relative variable fluorescence at the J-step and at the I-step
$M_0 = (\Delta V/\Delta t)_0 \approx 4 \text{ ms}^{-1} \cdot (F_{0.3ms} - F_{0.05ms})/F_v$	Initial slope of the O-J fluorescence rise
$S_m = \text{Area}/F_v$	Normalized area between the OJIP curve and the horizontal line at $F = F_m$
$N = S_m \cdot (M_0/V_J)$	Number of Q_A turnovers (i.e., Q_A reduction events from time 0 to that at F_m, t_{Fm})
Energy fluxes	
ABS	Photon flux absorbed by all PSII antenna pigments (absorption flux)
TR	Part of ABS trapped by active PSII leading to Q_A reduction
DI	Part of ABS dissipated, as heat, in PSII antenna in processes other than trapping
ET	Energy flux associated with electron transport from the reduced Q_A (Q_A^-) to the plastoquinone (PQ) pool
RE	Energy flux associated with electron transport from Q_A^- to PSI acceptor side
Specific energy fluxes per Q_A -reducing PSII reaction center (i.e., active PSII)	
$ABS/RC = (M_0/V_J)/(F_v/F_m)$	Absorption flux per active PSII (apparent PSII antenna size)
$TRo/RC = M_0/V_J$	Maximum trapped exciton flux per active PSII
$DIo/RC = ABS/RC - TRo/RC$	Energy flux dissipated per active PSII antenna in processes other than trapping
$ETo/RC = (M_0/V_J) \cdot (1 - V_J)$	Electron transport flux from Q_A^- to the PQ pool per active PSII
$REo/RC = (M_0/V_J) \cdot (1 - V_I)$	Electron transport flux from Q_A^- to the PSI end acceptors per active PSII
Quantum yields and efficiencies/probabilities	
$TRo/ABS = \phi_{Po} = F_v/F_m$	Maximum quantum yield of PSII photochemistry
$ETo/ABS = \phi_{Eo} = (F_v/F_m) \cdot (1 - V_J)$	Quantum yield of the electron flux from Q_A^- to the PQ pool
$REo/ABS = \phi_{Ro} = (F_v/F_m) \cdot (1 - V_I)$	Quantum yield of the electron flux from Q_A^- to PSI acceptor side
$ETo/TRo = \psi_{Eo} = 1 - V_J$	Efficiency of a trapped exciton to move an electron from Q_A^- to the PQ pool
$REo/TRo = \psi_{Ro} = 1 - V_I$	Efficiency of a trapped exciton to move an electron from Q_A^- to PSI acceptor side
$REo/ETo = \delta_{Ro} = (1 - V_I)/(1 - V_J)$	Efficiency to move an electron from a PQ reduced by Q_A^- at the Q_B -site to the PSI acceptor side
Performance indexes	
$Plabs = (RC/ABS) \cdot [\phi_{Po}/(1 - \phi_{Po})] \cdot [\psi_{Eo}/(1 - \psi_{Eo})]$	Performance index on absorption basis
$Pltotal = Plabs \cdot [\delta_{Ro}/(1 - \delta_{Ro})]$	Total performance index on absorption basis

(under post submergence drought) was picked as the least performing genotype (Figure S2). This contrasting pair of genotypes was used for further detailed characterization.

3.3 | Characterization of contrasting genotypes under stress and stress combinations (Experiment II)

Growth parameters, such as shoot length, root length, fresh weight, and dry weight, were higher in *Lomello* than in *C57-5043* across all the treatments (Figure 3A-T). Although the effect of combined heat

+drought and post-submergence drought was higher on all the growth traits measured for *Lomello* and *C57-5043*, *Lomello* maintained better growth across the treatments (Figure 3A-T; Figure S4). A comparative analysis of *Lomello* and *C57-5043* with known heat and drought tolerant check N22 and high-yielding elite cultivar IR64 further confirmed the superior performance of *Lomello* with higher values of growth traits (root-shoot length, fresh-dry weight), SPAD value and lower electrolyte leakage (Table S2; Figure S5). Electrolyte leakage was significantly higher in IR64 (14.2 to 97.3%) and N22 (12.3 to 88.6%) in comparison to *Lomello* (13.4 to 82.2%) across all the stress treatments.

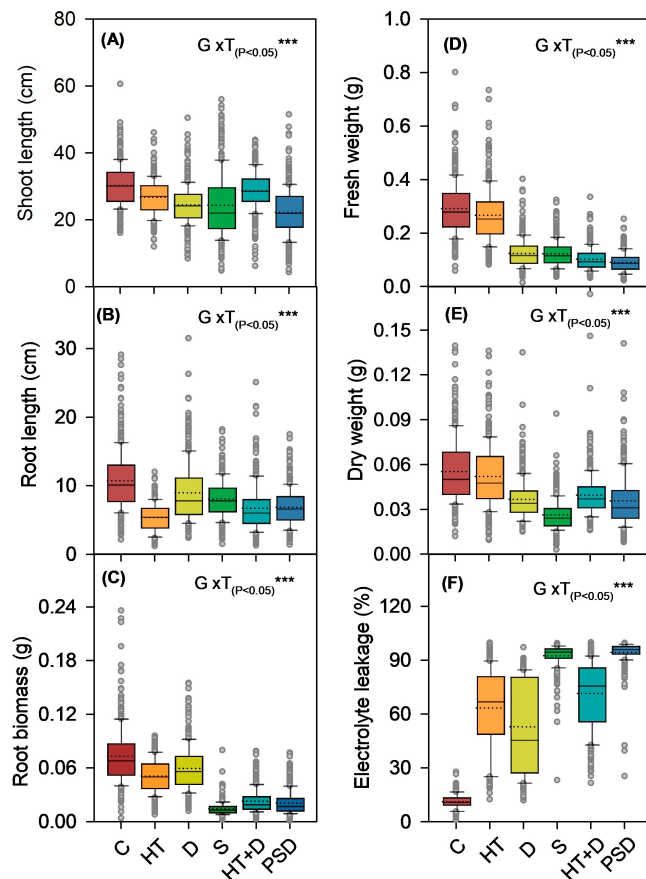


FIGURE 2 Phenotypic variations in the physiological traits of rice seedlings under individual, combined, and sequential stress. The box plots show variations in shoot length (A), root length (B), fresh root biomass (C), whole plant fresh weight (D), whole plant dry weight (E) and electrolyte leakage (F) of 394 rice genotypes exposed to individual, combined, and sequential stress during the year 2018. Within the box plots, solid and dotted lines represent the median and mean of the population, respectively. Box edges represent upper and lower quantiles, and the whiskers are for $1.5\times$ the quantile of the data. Outliers are shown as grey open circles. Levels of significance for genotype (G) and treatment (T) effects from ANOVA are given with Fisher's LSD value ($P < 0.05$). Significance: *** $P < 0.001$; Control [C], high temperature [HT], drought [D], combined high temperature and drought [HT + D], submergence [S], post submergence drought [PSD].

A significant reduction ($P < 0.001$) was observed in the leaf SPAD value (greenness index) in both *Lomello* and *C57-5043* under mild to severe exposure to different stress treatments (Figure 4 A-E). On the other hand, the quantum yield of PSII, as inferred from Chl *a* fluorescence (F_v/F_m), was significantly reduced (3.5 to 72.2%) across all the stress treatments. However, *Lomello* maintained a higher F_v/F_m ratio across the treatments, except post submergence drought (Figure 4F-J). Moreover, *Lomello* maintained a higher (3 to 57%) net photosynthetic rate (A), across the treatments. However, the magnitude of the difference was reduced under heat + drought and post-submergence drought stress (Figure 4K-O). Conversely, *Lomello* consistently maintained higher stomatal conductance and

transpiration rate, as compared to *C57-5043* across all the stress treatments (Figure 4P-Y), with relatively higher reduction noted under combined and sequential stress as compared to the individual stress (Figure 4P-Y).

3.4 | Chlorophyll fluorescence characteristics under individual stress and stress combinations

The time course of Chl *a* fluorescence transient, the OJIP curve, showed contrasting patterns for tolerant and sensitive genotypes across all the treatments, which also changed with the duration of the stress treatments (Figures 5 and S6). *Lomello* showed lower minimal fluorescence (F_o) but higher maximal fluorescence (F_m) values than *C57-5043* across all the stress treatments except HT + D. In *Lomello*, high temperature decreased F_m (maximal) and F_v (variable) levels with increasing duration of stress without affecting F_o . On the other hand, in *C57-5043*, F_o decreased by $\sim 33\%$, whereas F_m and F_v increased by $\sim 50\%$ under high temperature as compared to that in the controls (Figures 5 and S6). *Lomello*, as compared to *C57-5043*, showed a higher F_m/F_o ratio (reflecting higher PSII efficiency) under individual and combination of high temperature and drought stress conditions. Similarly, *Lomello* maintained a higher F_m/F_o ratio as compared to *C57-5043* under submergence and post-submergence drought stress conditions, particularly under severe stress conditions (Figures 5 and S6).

3.5 | Electron transport characteristics, based on chlorophyll *a* fluorescence measurement

The number of electron carriers in the linear electron transfer chain (from Q_A to ferredoxin, F_d) is reflected by S_m (the normalized area between the OJIP curve and the horizontal line at $F = F_m$) and N (the number of Q_A turnovers, i.e., Q_A reduction events from the time zero to that at F_{mt}) (Ferroni et al., 2022). A contrasting response was observed for S_m and N across the tolerant and sensitive genotypes under high temperature and drought stress treatments. *Lomello* showed a decrease, but *C57-5043* showed an increase in S_m and N , particularly under severe stress conditions (Figures S7 and S8). Moreover, the size of the PQ pool per PSII reaction centre (ET_o/RC) was smaller in *Lomello* as compared to that in *C57-5043*; however, it increased with the severity of stress across the genotypes (Figures S7 and S8). Additionally, *Lomello* showed a shorter t_{F_m} value (i.e., the time to reach F_m) under high temperature and drought stress as compared to *C57-5043*. On the other hand, S_m and N were substantially higher under high temperature + drought across the genotypes. However, *Lomello* maintained lower S_m , N and shorter t_{F_m} as compared to *C57-5043* (Figure 6A). Effect of submergence on S_m and N were relatively similar in both *Lomello* and *C57-5043* at the onset of stress exposure, but it increased significantly during the first four days of stress (mild stress), and then decreased over the next three days. Interestingly, under severe stress, i.e., when

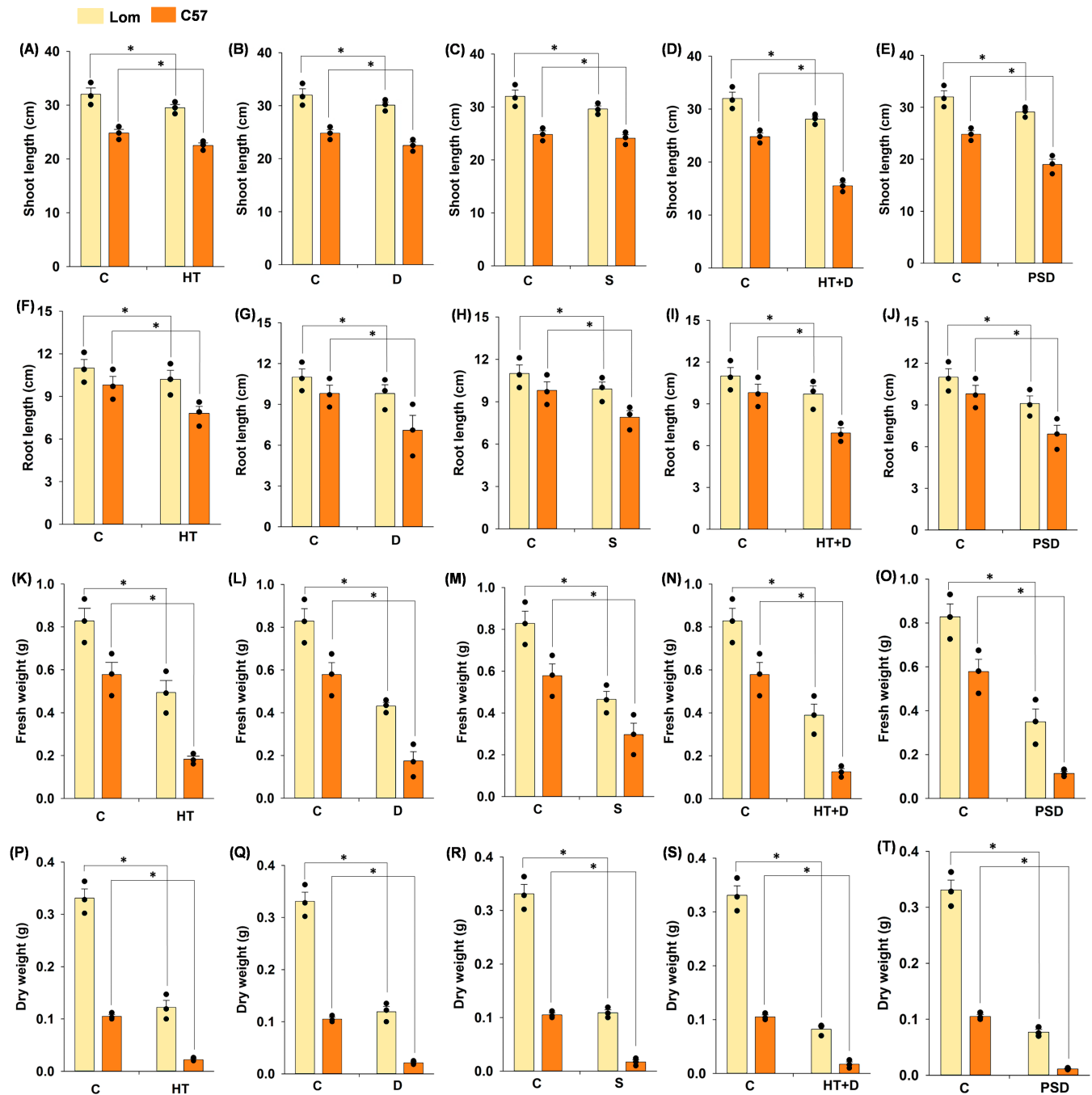


FIGURE 3 Effects of individual, combined and sequential stress on growth traits, i.e., shoot length [A-E], root length [F-J], whole plant fresh weight [K-O] and whole plant dry weight [P-T] of a contrasting set of rice genotypes Lom (*Lomello*) and C57 (*C57-5043*). Data are means (\pm SEM), $n = 3$ (where $n =$ number of biological replicates). Dots in each column represent the mean of observations taken at mild, moderate, and severe levels of stress. Corresponding measurements were taken from the respective controls against each stress. Significant differences for each genotype, compared with control conditions, were determined using Student's *t*-test: ($P < 0.05$); Control [C], high temperature [HT], drought [D], combined high temperature and drought [HT + D], submergence [S], post submergence drought [PSD].

submergence stress was extended up to 10 days, *Lomello* showed higher Sm and N values than *C57-5043* (Figure S9). On the other hand, Sm and N increased in both the genotypes under post submergence drought stress, with higher values noted for *Lomello* (36, 35, respectively) as compared to *C57-5043* (14, 19, respectively) (Figure 6B).

3.6 | Changes in the photosynthesis parameters related to PSII

Photosystem II antenna size is indicated by ABS/RC value, which was lower in *Lomello* as compared to *C57-5043*, when exposed to high temperature and drought stress. On the contrary, ABS/RC value, in

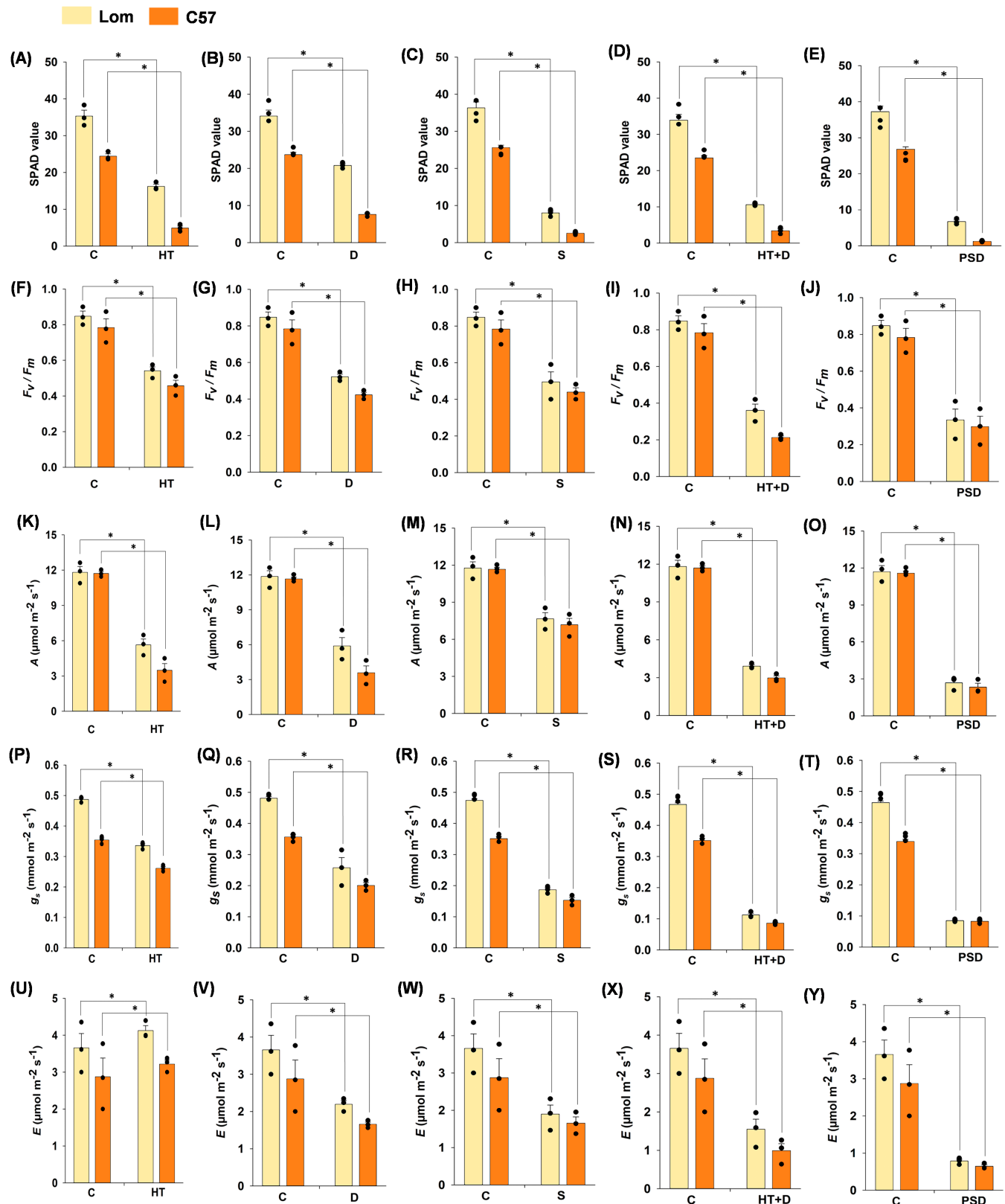


FIGURE 4 Effects of individual, combined and sequential stress on leaf chlorophyll index (SPAD value) [A-E], chlorophyll a fluorescence (F_v/F_m ratio) [F-J], net photosynthesis rate (A) [K-O], stomatal conductance (g_s) [P-T] and transpiration rate (E) [U-Y] in a contrasting set of rice genotypes Lom (*Lomello*) and C57 (C57-5043). Data are means (\pm SEM), $n = 3$ (where $n =$ number of biological replicates consisting of one plant). Dots in each column represent the mean of observations taken at mild, moderate, and severe levels of stress. Corresponding observations were taken from the respective controls against each stress. Significant differences for each genotype compared with control conditions were determined using Student's *t*-test: ($P < 0.05$); Control [C], high temperature [HT], drought [D], combined high temperature and drought [HT + D], submergence [S], post submergence drought [PSD].

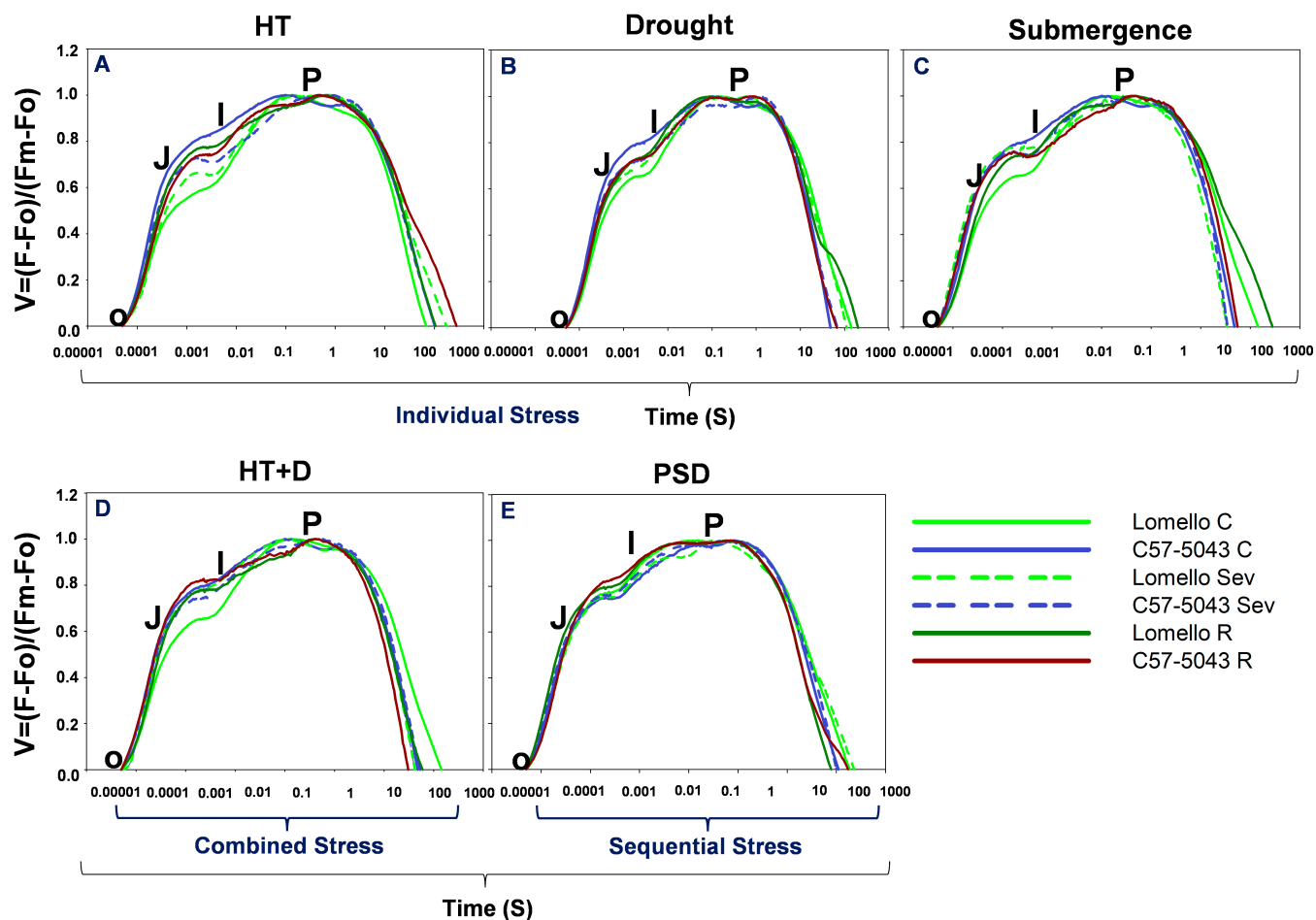


FIGURE 5 Chlorophyll a fluorescence transient rise (the OJIP curve) for the best (*Lomello*) and least performing rice genotypes showing changes under combined and sequential stress. Data for the most tolerant (*Lomello*, green color) and the most sensitive (*C57-5043*, red color) rice genotype—kept under individual, combined, or sequential stress conditions. *Abbreviations*: HT - high temperature; D - drought; S - submergence; HT + D - high temperature and drought and PSD - post submergence drought. C - control, Sev- severe stress, R - recovery.

C57-5043, is highest at the onset of stress, but gradually declines with increased duration of stress (Figures S7 and S8). Under combined high temperature + drought stress, ABS/RC gradually increased with stress severity across both the genotypes (Figure 6A). ABS/RC also increased gradually with the severity of stress under submergence for both genotypes (Figure S9). Conversely, ABS/RC remained low under the post submergence drought stress across all the genotypes, in contrast to the high values observed under submergence stress (Figure 6B). TRo/RC (= Mo/V_j) is a measure of the maximum trapped exciton flux per active PSII leading to Q_A reduction (Table 1). We observed that *C57-5043* showed higher responses for TRo/RC values under high temperature and drought stress (Figures S7 and S8). Conversely, the TRo/RC value in *Lomello* increased under high temperature + drought stress with the progression of stress but abruptly decreased under severe stress conditions. On the contrary, the TRo/RC value in *C57-5043* did not change substantially under high temperature + drought stress period and remained at moderate levels (Figure 6A). Under submergence stress, TRo/RC values increased gradually with the duration of stress across the genotypes, with lower values noted for *Lomello* (Figure S9). On the other hand, during the post-submergence drought stress, TRo/RC values

decreased with the duration of stress in *Lomello*, but *C57-5043* did not show any substantial change in TRo/RC (Figure 6B).

Dlo/RC represents the specific dissipated energy flux (Table 1). *Lomello* maintained low Dlo/RC values under high temperature and drought as compared to *C57-5043* at the onset of mild stress (Figures S7 and S8). However, *C57-5043* showed lower Dlo/RC values as compared to *Lomello* under combined high temperature + drought stress, which had a very high Dlo/RC value in the middle of stress exposure and declined abruptly thereafter. Under submergence and post-submergence drought conditions, Dlo/RC was also generally lower in *Lomello* compared to *C57-5043*; while it increased significantly under severe submergence stress (particularly in *C57-5043*), it remained relatively constant during the mild, moderate, and severe post submergence drought conditions (Figure 6B).

3.7 | Changes in the linear electron transport

Considering that ET_o/RC, ET_o/ABS, and ET_o/TR_o values are directly proportional to (1 - V_j) (Table 1), V_j was observed to be lower in

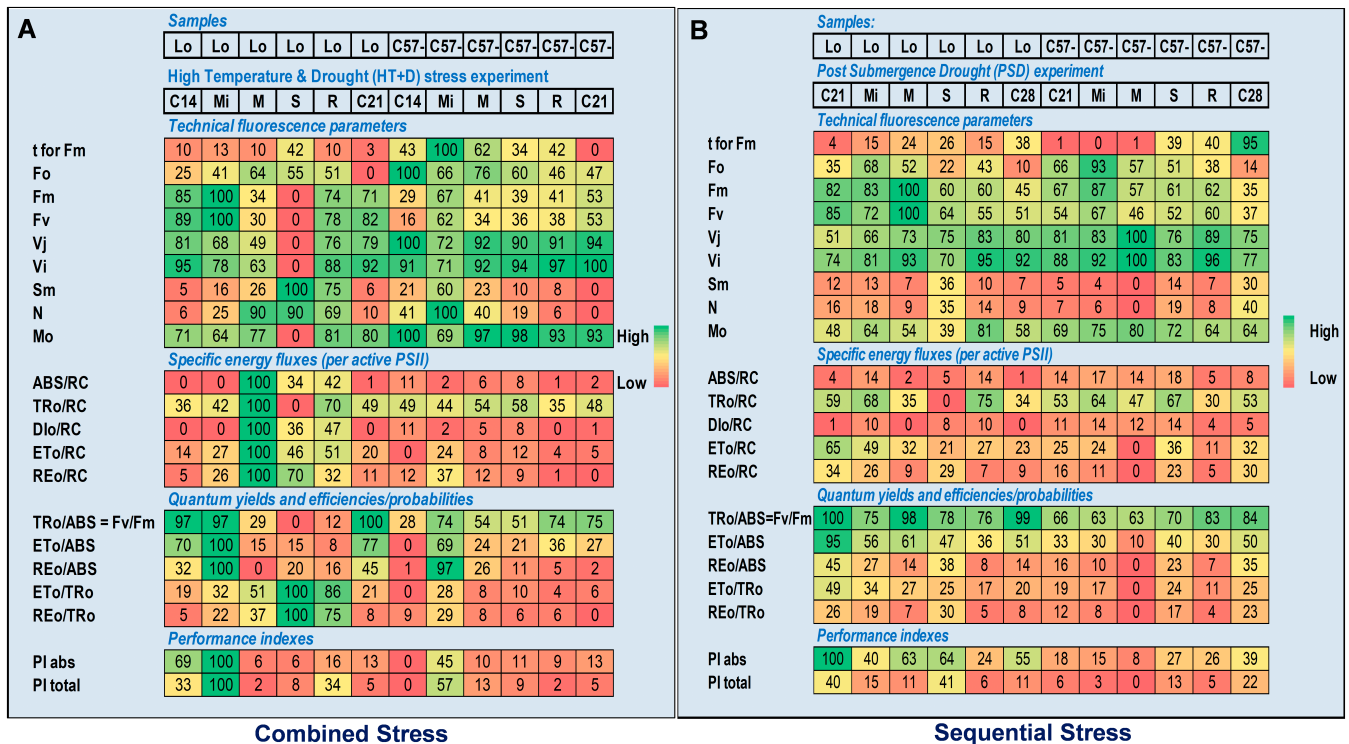


FIGURE 6 Handy Pea parameters for the best (*Lomello*) and the least (*C57-5043*) performing rice genotypes showing changes under combined and sequential stress. Heat map representing Chl *a* fluorescence parameters of the most tolerant *Lomello* (Lo) and most sensitive *C57-5043* (C57) rice genotypes, calculated from the OJIP fluorescence induction transients of samples, which were exposed to combined high temperature and drought (HT + D) and post submergence drought (PSD) i.e., submergence stress followed by drought stress. The fluorescence parameters were calculated for the following samples: C14, C21, and C28 - Control samples grown 14, 21, and 28 days under 28/23°C day/night, and 65–70% relative humidity (see Material and Methods); (A): For combined stress; Mi, M, and S - 14 days samples exposed to 35/29°C day/night and to withheld watering until 80% soil water content SWC (Mild stress), 60% SWC (Moderate stress), 40% SWC (Severe stress). (B): For sequential stress; 14 days old seedlings were completely submerged in a water tank for 7 days and after that subjected to drought conditions by withholding water until 80% soil water content SWC (Mild stress), 60% SWC (Moderate stress), 40% SWC (Severe stress), and after three hours Recovery following the Severe stress (R).

Lomello as compared to that in *C57-5043* across all the stress conditions (Figure 6A, B; Supplementary Figures S7–S8). Based on this, *Lomello* must have had a higher flux of electrons from the reduced Q_A to the PQ pool (Strasser et al., 1995) across all the stress conditions. On the contrary, *C57-5043* had lower values of the parameters related to the energy flux ETo, and were interpreted to have a higher fraction of Q_B -nonreducing PSII centres with higher Mo and V_j across all the stress conditions (Figure 6; Supplementary Figures S7 and S8). Parameters such as REo/RC, REo/ABS, and REo/TRo were differentially affected across stress treatments (Figures 6; Figures S7 and S8). Under high-temperature stress, these parameters had lower values in *Lomello* as compared to *C57-5043*, which is associated with higher V_i (relative variable fluorescence at the I-step) levels observed in both genotypes, indicating inhibition of the (electron) acceptor side of PSII and relative change in the proportion of Q_B -non-reducing PSII RCs (Figure S7; Setlik et al., 1990). Moreover, values of these parameters were very high in *Lomello*, as compared to *C57-5043* under high temperature and drought conditions, indicating greater photoinactivation of PSII (Figures S7 and S8). On the contrary, during the combined high temperature + drought stress, submergence and post-submergence

drought conditions, the parameters related to the energy flux REo were higher in *Lomello* as compared to *C57-5043* (Figures 6B and S9). The observed increase of REo/RC, REo/ABS, and REo/TRo with the severity of stress particularly observed under high temperature and drought conditions (Figures S7 and S8) suggests a preferential inactivation of PSII centers compared to PSI centers due to photoinactivation (Setlik et al., 1990).

3.8 | Changes in the performance index

Lomello had substantially higher values of performance index on absorption basis (Plabs) and total performance index on absorption basis (PI_{total}) as compared to *C57-5043* under individual high temperature and drought stress (Supplementary Table S3; Supplementary Figures S7 and S8). However, Plabs and PI_{total} were considerably lower across the genotypes under high temperature + drought stress (Figure 6A). Further, variable response was noted for Plabs and PI_{total} under submergence stress across the genotypes (Supplementary Figure S9). However, *Lomello* showed higher Plabs and PI_{total} values

under post submergence drought as compared to C57-5043 (Figure 6B).

4 | DISCUSSION

Considering that there are no multiple abiotic stress-tolerant donors reported in rice and other cereal crops, a major objective of this study was to phenotype and screen potential genotype(s) that show tolerance to multiple abiotic stresses. Moreover, understanding the basis of resilience to more than one stress is crucial for further characterization of genotypes to delineate the mechanistic basis of multiple stress tolerance. The effect of stress on different phenotypic traits may vary greatly based on the escape, avoidance and cellular level tolerance in the plants (Bahuguna et al., 2015; Yadav et al., 2022). Therefore, it is necessary to understand how plants deal with individual stress and respond when the stressor changes (Jangale et al., 2019; Joshi et al., 2020; Yadav et al., 2022). We observed key traits, particularly at the early growth (seedling) stage, that are responsive to mild, moderate and severe stress (of different types) along with a recovery window. Interestingly, adaptive plasticity in some traits, such as root length, transpiration, and stomatal conductance, could help in avoiding heat or drought stress but may not work under stress combinations (Suzuki et al., 2014; Yadav et al., 2022). Considering that the ability of a genotype to maintain photosynthesis and growth at the early developmental phase is pivotal, we measured different fluorescence parameters to assess the integrity of photosynthetic machinery and its efficiency across the stressors. Following a screening of 394 diverse rice genotypes at the seedling stage, the two most contrasting *Japonica* genotypes were selected for studying photosynthetic characteristics. The major findings of the study are as follows.

4.1 | Genetic response to individual and stress combination

Growth traits such as fresh weight, dry weight, root length, shoot length and root biomass of 394 rice genotypes showed variable responses to each stressor (Figure 2). Moreover, tissue damage measured as electrolyte leakage showed substantial variations across the stresses (Figure 2). In general, the effect of stress combinations on growth traits and electrolyte leakage was significantly higher across the genotypes as compared to individual stresses (Figure 2). It has been reported previously that stress combinations are generally more detrimental to growth and yield (Mittler, 2006; Suzuki et al., 2014; Yadav et al., 2022). Previous studies demonstrated that the ability to avoid stress, such as HT by transpirational cooling and water deficit by stomatal closure, may not be effective under stress combination (e.g. H + D) (Yadav et al., 2022). Moreover, Mittler (2006) and Anwar et al., (2022) have emphasized that a differential pattern at the transcriptome, metabolome and proteome levels indicates a characteristic pattern under stress combinations that involves a distinct set of

genes, proteins and metabolites. Nevertheless, the mechanistic basis of genetic response to stress combination is not yet well understood.

A performance index, calculated on the basis of growth and electrolyte leakage, revealed *Lomello* as the best-performing and C57-5043 as the least-performing genotype across the individual and combination stresses (Supplementary Figure S2, S3). The effect of stressors on the growth traits of *Lomello* and C57-5043 showed that *Lomello* consistently performed better across all the stress treatments (Figure 3; Supplementary Figure S4; Supplementary Table S2). A comparative analysis of *Lomello* and C57-5043 with N22 (heat and drought tolerant check) and elite rice cultivar IR64 further confirmed *Lomello* to be the best-performing genotype (Supplementary Figure S5) across the stress treatments. In order to understand the resilience of *Lomello* across the stress conditions at the early vegetative stage, we studied photosynthesis and associated traits since the ability to maintain high photosynthesis is a potential marker for determining the overall health of the genotypes (Kromdijk et al., 2016; Ort et al., 2022). A decline in chlorophyll (SPAD value), chlorophyll a fluorescence (Fv/Fm) and gas exchange traits were consistent across the stress treatments, with significantly higher reductions observed for C57-5043 across the stresses (Figure 4). Inhibition of photosynthesis may result from stomatal as well as non-stomatal limitations (Farquhar & Sharkey, 1982). While stomatal limitation could be dominant under mild stress, drastic reduction in photosynthesis under stress combinations could be due to both stomatal and non-stomatal limitation (damage to chlorophyll and components of photosynthesis machinery) (Oneto et al., 2016; Wungrampha et al., 2019; Liu et al., 2019). Besides, net photosynthetic rate, stomatal conductance and transpiration have been suggested to be important traits for heat and drought avoidance (Bahuguna et al., 2015; Kadam et al., 2017). Moreover, a faster response of stomatal conductance can be an effective adaptive trait for rice under transition from mild to severe drought conditions (Qu et al., 2016). Reduced stomatal conductance and transpiration rates make plants vulnerable due to rise in tissue temperature under stress combinations such as high temperature + drought in the absence of evaporative cooling of the leaf surface (Kadam et al., 2015; Yadav et al., 2022). Thus, temperature-induced damage could be significantly higher under combined high temperature + drought stress. Although these traits showed higher reductions under stress combinations, *Lomello* was able to maintain a lower reduction in gas exchange traits and chlorophyll a fluorescence across the stress conditions (Figure 4), which could be plausibly due to a robust antioxidant defence system (resulting in low electrolyte leakage) and photosystem stability. This eventually must have allowed *Lomello* to maintain higher photosynthesis as the stomatal closure under drought or heat+drought could reduce the availability of CO₂ (Oneto et al., 2016; Ibrahim et al., 2019). Indeed, the selection of genotypes having robust photosynthesis machinery and the ability to fix more carbon per unit area and time could compensate for carbon losses under stress and maintain higher yield under optimum conditions (Driever et al., 2014; Long et al., 2015; Bahuguna et al., 2022). However, further research is warranted to confirm the tissue-level resilience of *Lomello* at the reproductive and grain-filling stage.

4.2 | Robust photosynthetic machinery in *Lomello* helps it survive under multiple stresses

The maximum quantum yield of PSII photochemistry (measured as Fv/Fm) is a parameter providing information on the capacity of the plant to use the light energy absorbed by the PSII antenna in the photochemical processes in dark-adapted samples (Shu et al., 2016). *Lomello* consistently showed a significantly higher Fv/Fm ratio as compared to C57-5043 across all the treatments and severity levels of stress (Figures 5 and S6). Further, our results show that the combined high temperature + drought stress led to a drastic reduction in photosynthesis in sensitive genotype C57-5043, as evidenced by a significant decrease in Fv/Fm (Figures 4 and 5). This reduction in Fv/Fm was accompanied by an increase in F_o, the minimal fluorescence (Figure 6; Figures S7-9). These observations in C57-504 suggest an inactivation of a large fraction of PSIIs under the combined stress, as well as a blockage in electron transfer in PSII from the primary (electron) acceptor plastoquinone (Q_A) to the secondary (electron) acceptor plastoquinone (Q_B) (Mehta et al., 2010). On the other hand, a substantial impact of submergence and post-submergence drought stress has been observed on gas exchange traits and photosynthesis machinery in this genotype (Figure 4). Morales et al. (2022) have shown that drastic reduction in light intensity, stomatal conductance, and photosynthesis resulted in severe energy and carbon imbalance in *Arabidopsis* under submergence stress and post-submergence drought stress. Yeung et al. (2018) further demonstrated how the post-submergence phase is associated with new stressors. In this phase, plant tissues acclimated to submergence-associated low light and hypoxia often experience physiological drought stress due to impaired root hydraulics and/or leaf water loss. Moreover, following de-submergence, a rapid and greater accumulation of reactive oxygen species has been shown in a sensitive *Arabidopsis* accession. In our study, this is in line with the severe photoinhibition observed in both genotypes, particularly in C57-5043 during the post-submergence recovery phase (Figures 4, 6; S7-S9). Photosynthetic assimilation and electron transport are the key factors known to influence the growth as well as the yield of plants (Demirel et al., 2020). The higher Fv/Fm ratio and associated chlorophyll fluorescence parameters in *Lomello*, observed in our work (Figures 6; S7-S9), are in line with the ability to maintain higher photosynthesis under heat, drought, and submergence, suggesting that maintaining the functionality of photosynthesis machinery is essential for stress tolerance, in addition to a tight regulation of reactive oxygen species production, and reactive oxygen species induced damage in the cell (Foyer and Shigeoka 2011). Indeed, *Lomello* acclimated to different stress exposures by its ability to reduce the light-harvesting capacity, therefore minimizing the potential for cellular damage resulting from the production of excessive reactive oxygen species during the photosynthetic electron transport (Figures 6; S7-S9). This adaptation strategy could be useful for avoiding irreversible photodamage during oxidative bursts under abiotic stress conditions as well (Kromdijk et al., 2016; Soda et al., 2018; Wungrampha et al., 2019).

Our data on chlorophyll fluorescence parameters indicate that PSII inactivation, under stress across the genotypes, leads to a

substantially higher fraction of Q_A-nonreducing centres, Q_B-nonreducing PSII centres, and a larger PQ pool size in sensitive genotype C57-5043 (Figures 6; S7-S9). Conversely, the observed ABS/RC values indicate a smaller PSII antenna size in *Lomello* compared to that in C57-5043 under both control and stress conditions (Figures 6; S7-S9). This could give *Lomello* an advantage in reducing oxidative damage and maintaining higher photosynthesis due to less prone photosynthesis machinery (Sayre et al., 2020). Further, parameters characterizing the energy flux related to the electron transport from the reduced Q_A (Q_A⁻) to the PQ pool (i.e., ETo/RC, ETo/ABS, and ETo/TRo) were substantially higher in *Lomello* across all the stress treatments. On the other hand, the JIP parameters, characterizing the electron transport from Q_A⁻ to the acceptor side of PSI (i.e., REo/RC, REo/ABS, and REo/TRo), revealed a lower sensitivity of PSI, compared to that of PSII, to the stress conditions. Moreover, a striking suppression of the JIP phase in OJIP transients was observed under stress conditions, which is plausibly due to the maintenance of the redox poise of the PQ pool or hindrance in the electron flow (Gautam et al., 2014). A higher performance index, Plabs and Pl_{total}, observed in *Lomello*, is in line with a higher Fv/Fm ratio (Figures 6; S7-S9; Table S3), and an increase in Dlo/RC in *Lomello* further confirms the dissipation of excess absorbed light through reaction centers as well as antenna under severe stress leading to a decrease in photochemical reactions. Our study explains the ability of *Lomello* to maintain Chl a fluorescence parameter that ensures better functionality of PSII centers and non-linear electron transport, which keeps reactive oxygen species (ROS) accumulation under check in its chloroplasts (Bacarin et al. 2016). In *Lomello*, a higher membrane stability and an increased amount of leaf chlorophyll may be due to a better management of ROS during all the stress conditions. Further, the cumulative effect of higher photosystem stability, increased rate of electron transfer, and greater efficiency of alternate electron acceptors provide a major sink for ROS by reducing the possibility of electron transfer to molecular oxygen in the chloroplast (see, e.g., Foyer and Noctor 2003, Silva et al. 2010; Bahuguna et al., 2015). Moreover, this higher rate of photosynthesis under stress is expected to reduce the possibility of H₂O₂ production through the photorespiratory pathway (see, e.g., Apel and Hirt, 2004), contributing to the lowering of ROS-induced damage in *Lomello* under stress conditions. On the other hand, the stress response in plants is always accompanied by reprogramming of the metabolism from the photo-assimilatory to the survival pathway (Chojak-Kozniowska et al., 2017). Although previous studies have shown detrimental effects of combined stress combinations in crops such as rice (Kadam et al., 2015; Morlaes et al., 2022; Yadav et al., 2022), yet the response of rice to sequential post-submergence drought stress is unique. For example, submergence regulator SUB1A cross-talk across submergence and drought stress in rice where SUB1A has been shown to augment ABA responsiveness and ROS scavenging enzymes, hence working efficiently across submergence and drought stress at the vegetative stage (Fukao et al., 2011). Therefore, the superior performance of *Lomello* under stress combinations such as post-submergence drought could provide opportunities to identify novel molecular mechanisms that protect plants from cellular-

level damage. Nevertheless, a relatively higher impact of combination and sequential stress on growth traits and photosynthetic machinery across the genotypes suggests further systematic investigation of other stress tolerance mechanisms across different (sensitive) growth stages. Phenotyping key photosynthetic traits in a diverse and large set of genotypes could help in the identification of novel QTLs and genes by association mapping. However, the lack of phenotyping facilities for screening and characterization of a large number of genotypes across different stress environments is a major bottleneck. Recent advancements in high-throughput phenotyping platforms integrated with artificial intelligence could allow the phenotyping of a large set of genotypes across growth stages, such as reproductive and grain filling, which will expedite crop improvement through integrating complex photosynthetic traits in the breeding programs.

The present study is a first attempt to analyze detailed photosynthesis-related parameters and to examine Chl *a* fluorescence profile associated with the complex adaptive processes in rice under individual, combined and sequential stresses. Results obtained in this study support our hypothesis that the photosynthesis activity is differentially regulated under individual, combined and sequential abiotic stresses and also with respect to the genotype and the severity of the stress. The response of contrasting genotypes to individual, combined and sequential abiotic stresses highlights the plasticity of the rice genome and its ability to modulate its response to complex environmental conditions. This study has revealed that regulating the equilibrium between the photosynthetic electron transport chain and gas exchange during fluctuating climatic conditions may help in acclimating under stressful environments. Further studies on genetic regulation of cellular and metabolic processes across individual and combination stresses are expected to achieve the breakthroughs required for the development of climate-resilient crops.

AUTHOR CONTRIBUTIONS

The idea of the study was conceptualized by A.P; K.A and R.J did the experiments; K.A and R.N.B participated in data analysis and interpretations; K.A., R.N.B. and R.J wrote the manuscript; G.G., R.S., S.L.S.P. and A.P. participated in the writing and editing the manuscript. All authors have read and agreed to the final draft of the manuscript.

ACKNOWLEDGEMENTS

This research was supported by the Department of Biotechnology, Government of India, a joint Indo-NWO project, Indo-US Science and Technology Forum (IUSSTF) through Indo-US Advanced Bioenergy Consortium (IUABC), International Atomic Energy Agency (Vienna), and Institutional Umbrella support under DST-FIST and PURSE; UGC-UPEII, DRS and Networking. Govindjee thanks the staff (Jeffrey Haas and his associates) of the Office of Information Technology, Life Sciences, University of Illinois at Urbana-Champaign, for help with computer-related work.

FUNDING INFORMATION

Department of Biotechnology, Government of India, for the Indo-NWO Project (# BT/IN/NWO/15/AP/2015-16).

CONFLICTS OF INTEREST STATEMENT

Authors declare that there is no conflict of interest among them.

DATA AVAILABILITY STATEMENT

Data sharing is not applicable to this article as all created data is already contained within this article.

ORCID

Rohit Joshi  <https://orcid.org/0000-0002-6524-4722>

Rajeev N. Bahuguna  <https://orcid.org/0000-0002-6249-5833>

Govindjee Govindjee  <https://orcid.org/0000-0003-3774-0638>

Rashmi Sasidharan  <https://orcid.org/0000-0002-6940-0657>

Sneh L. Singla-Pareek  <https://orcid.org/0000-0002-0521-2622>

Ashwani Pareek  <https://orcid.org/0000-0002-2923-0681>

REFERENCES

- Anwar K, Joshi R, Dhankher OP, Singla-Pareek SL, Pareek A (2021) Elucidating the Response of Crop Plants towards Individual, Combined and Sequentially Occurring Abiotic Stresses. *International Journal of Molecular Sciences* 22(11): 6119.
- Anwar K, Joshi R, Morales A, Das G, Yin X, Anten NP, Raghuvanshi S, Bahuguna RN, Singh MP, Singh RK, van Zanten M, Sasidharan R, Singla-Pareek SL, Pareek A (2022) Genetic diversity reveals synergistic interaction between yield components could improve the sink size and yield in rice. *Food and Energy Security* 11(2): e334.
- Apel K, Hirt H (2004) Reactive oxygen species: metabolism, oxidative stress, and signal transduction. *Annual Review of Plant Biology* 55: 373–99.
- Bacarin MA, Martinazzo EG, Cassol D, Falqueto AR, Silva DM (2016) Daytime variations of chlorophyll *a* fluorescence in pau d'alto seedlings. *Revista Arvore* 40(6): 1023–30.
- Bahuguna RN, Chaturvedi AK, Pal M, Viswanathan C, Jagadish SVK, Pareek A (2022) Carbon dioxide responsiveness mitigates rice yield loss under high night temperature. *Plant Physiology* 188(1): 285–300.
- Bahuguna RN, Jha J, Pal M, Shah D, Lawas LM, Khetarpal S, Jagadish SVK (2015) Physiological and biochemical characterization of NERICA-L-44: a novel source of heat tolerance at the vegetative and reproductive stages in rice. *Physiologia Plantarum* 154(4): 543–59.
- Bailey-Serres J, Fukao T, Ronald P, Ismail A, Heuer S, Mackill D (2010) Submergence tolerant rice: SUB1's journey from landrace to modern cultivar. *Rice* 3: 138–147.
- Bailey-Serres J, Cho-Lee S, Brinton E (2012) Waterproofing crops: effective flooding survival strategies. *Plant Physiology* 160(4): 1698–1709.
- Chojak-Kozniowska J, Linkiewicz A, Sowa S, Radzich MA, Kuzniak E (2017) Interactive effects of salt stress and *Pseudomonas syringae* pv. *lachrymans* infection in cucumber: Involvement of antioxidant enzymes, abscisic acid and salicylic acid. *Environmental and Experimental Botany* 136: 9–20.
- Choudhury FK, Rivero RM, Blumwald E, Mittler R (2017) Reactive oxygen species, abiotic stress and stress combination. *Plant Journal* 90(5): 856–867.
- Coolen S, Proietti S, Hickman R, Davila-Olivas NH, Huang PP, Van-Verk MC, Van Pelt JA, Wittenberg AHJ, De-Vos M, Prins M, Van Loon JJ, Aarts MG, Dicke M, Pieterse CM, Van Wees SC (2016) Transcriptome dynamics of Arabidopsis during sequential biotic and abiotic stresses. *Plant Journal* 86(3): 249–67.
- De Kort H, Prunier JG, Ducatez S, Honnay O, Baguette M, Stevens VM, Blanchet S (2021) Life history, climate and biogeography interactively affect worldwide genetic diversity of plant and animal populations. *Nature Communications* 12(1): 516.
- Demirel U, Morris WL, Ducreux LJ, Yavuz C, Asim A, Tindas I, Campbell R, Morris JA, Verrall SR, Hedley PE, Gokce ZNO, Caliskan S, Aksoy E,

- Caliskan ME, Taylor MA, Hancock RD (2020) Physiological, Biochemical, and Transcriptional Responses to Single and Combined Abiotic Stress in Stress-Tolerant and Stress-Sensitive Potato Genotypes. *Frontier in Plant Science* 11: 169.
- Driever SM, Lawson T, Andralojc PJ, Raines CA, Parry MAJ (2014) Natural variation in photosynthetic capacity, growth, and yield in 64 field-grown wheat genotypes. *Journal of Experimental Botany* 65(17): 4959–4973.
- Eliazer-Nelson ARL, Ravichandran K, Antony U (2019) The impact of the Green Revolution on indigenous crops of India. *Journal of Ethnic Foods* 6(1): 8.
- Farquhar GD, Sharkey TD (1982) Stomatal Conductance and Photosynthesis. *Annual Review Plant Physiology* 33: 317–345.
- Ferroni L, Živčák M, Kovar M, Colpo A, Pancaldi S, Allakhverdiev SI, Brestič M (2022) Fast chlorophyll *a* fluorescence induction (OJIP) phenotyping of chlorophyll-deficient wheat suggests that an enlarged acceptor pool size of Photosystem I helps compensate for a deregulated photosynthetic electron flow. *Journal of Photochemistry and Photobiology B Biology* 234: 112549.
- Foyer CH, Shigeoka S (2011) Understanding Oxidative Stress and Antioxidant Functions to Enhance Photosynthesis. *Plant physiology* 155(1): 93–100.
- Foyer CH, Neukermans J, Queval G, Noctor G, Harbinson J (2012) Photosynthetic control of electron transport and the regulation of gene expression. *Journal of Experimental Botany* 63(4): 1637–1661.
- Foyer CH, Noctor G (2003) Redox sensing and signalling associated with reactive oxygen in chloroplasts, peroxisomes and mitochondria. *Physiologia Plantarum* 119(3): 355–364.
- Fukao T, Yeung E, Bailey-Serres J (2011) The submergence tolerance regulator SUB1A mediates crosstalk between submergence and drought tolerance in rice. *Plant Cell* 23(1): 412–27.
- Gautam A, Agrawal D, SaiPrasad SV, Jajoo A (2014) A quick method to screen high and low yielding wheat cultivars exposed to high temperature. *Physiology and Molecular Biology of Plants* 20(4): 533–7.
- Grassini P, Eskridge KM, Cassman KG (2013) Distinguishing between yield advances and yield plateaus in historical crop production trends. *Nature Communications* 4: 2918.
- Ibrahim W, Zhu YM, Chen Y, Qiu CW, Zhu S, Wu F (2019) Genotypic differences in leaf secondary metabolism, plant hormones and yield under alone and combined stress of drought and salinity in cotton genotypes. *Physiologia Plantarum* 165(2): 343–355.
- Jagadish SVK, Muthurajan R, Oane R, Wheeler TR, Heuer S, Bennett J, Craufurd PQ (2010) Physiological and proteomic approaches to address heat tolerance during anthesis in rice (*Oryza sativa* L.). *Journal of Experimental Botany* 61(1): 143–156.
- Jangale BL, Chaudhari RS, Azeez A, Sane PV, Sane AP, Krishna B (2019) Independent and combined abiotic stresses affect the physiology and expression patterns of DREB genes differently in stress-susceptible and resistant genotypes of banana. *Physiologia Plantarum* 165(2): 303–318.
- Joshi R, Sahoo KK, Tripathi AK, Kumar R, Gupta BK, Pareek A, Singla-Pareek SL (2018) Knockdown of an inflorescence meristem-specific cytokinin oxidase–OsCKX2 in rice reduces yield penalty under salinity stress condition. *Plant Cell & Environment* 41(5): 936–946.
- Joshi R, Sahoo KK, Singh AK, Anwar K, Pundir P, Gautam RK, Krishnamurthy SL, Sopory SK, Pareek A, Singla-Pareek SL (2020) Enhancing trehalose biosynthesis improves yield potential in marker-free transgenic rice under drought, saline, and sodic conditions. *Journal of Experimental Botany* 71(2): 653–668.
- Kadam NN, Yin X, Bindrabn PS, Struik PC, Jagadish KSV (2015) Does morphological and anatomical plasticity during the vegetative stage make wheat more tolerant of water deficit stress than rice? *Plant Physiology* 167(4): 1389–1401.
- Kadam NN, Tamilselvan A, Lawas LMF, Quinones C, Bahuguna RN, Thomson MJ, Dingkuhn M, Muthurajan R, Struik PC, Yin X, Jagadish SVK (2017) Genetic Control of Plasticity in Root Morphology and Anatomy of Rice in Response to Water Deficit. *Plant Physiology* 174(4): 2302–2315.
- Kobayashi E, Suzuki T, Funayama R, Nagashima T, Hayashi M, Sekine H, Tanaka N, Moriguchi T, Motohashi H, Nakayam K, Yamamoto M (2016) Nrf2 suppresses macrophage inflammatory response by blocking proinflammatory cytokine transcription. *Nature Communications* 7: 11624.
- Kromdijk J, Glowacka K, Leonelli L, Gabilly ST, Iwai M, Niyogi KK, Long SP (2016) Improving photosynthesis and crop productivity by accelerating recovery from photoprotection. *Science* 354(6314): 857–861.
- Lakra N, Kaur C, Anwar K, Singla-Pareek SL, Pareek A (2018) Proteomics of contrasting rice genotypes: Identification of potential targets for raising crops for saline environment. *Plant Cell & Environment* 41(5): 947–969.
- Liu J, Zhao Y, Song H, Chen J, Long Y (2019) Antagonism or synergism? Combined effects of enhanced UV-B radiation and acid rain on photosynthesis in seedlings of two C4 plants. *Acta Ecologica Sinica* 40(1): 72–80.
- Long SP, Marshall-Colon A, Zhu XG (2015) Meeting the Global Food Demand of the Future by Engineering Crop Photosynthesis and Yield Potential. *Cell* 161(1): 56–66.
- Loudet O, Hasegawa PM (2017) Abiotic stress, stress combinations and crop improvement potential. *Plant Journal* 90(5): 837–838.
- McClung CR (2006) Plant Circadian Rhythms. *Plant Cell* 18(4): 792–803.
- Mehta P, Jajoo A, Mathur S, Bharti S (2010) Chlorophyll *a* fluorescence study revealing effects of high salt stress on Photosystem II in wheat leaves. *Plant Physiology and Biochemistry* 48(1): 16–20.
- Mittler R (2006) Abiotic Stress, the Field Environment and Stress Combination. *Trends in Plant Science* 11(1): 15–9.
- Morales A, de Boer HJ, Douma JC, Elsen S, Engels S, Glimmerveen T, Sajeev N, Huber M, Luimes M, Luitjens E, Raatjes K, Hsieh C, Teapal J, Wildenbeest T, Jiang Z, Pareek A, Singla-Pareek SL, Yin X, Evers J, Anten NPR, van Zanten M, Sasidharan R (2022) Effects of sublethal single, simultaneous and sequential abiotic stresses on phenotypic traits of Arabidopsis thaliana. *AoB Plants* 14(4): plac029.
- Munoz P, Munne-Bosch S (2017) Photo-Oxidative Stress during Leaf, Flower and Fruit Development. *Plant Physiology* 176(2): 1004–1014.
- Nishiyama Y, Murata N (2014) Revised scheme for the mechanism of photoinhibition and its application to enhance the abiotic stress tolerance of the photosynthetic machinery. *Applied Microbiology and Biotechnology* 98(21): 8777–8796.
- Oneto CD, Otegui ME, Baroli I, Beznec A, Faccio P, Bossio E, Blumwald E, Lewi D (2016) Water deficit stress tolerance in maize conferred by expression of an isopentenyltransferase (IPT) gene driven by a stress- and maturation-induced promoter. *Journal of Biotechnology* 220: 66–77.
- Ort DR, Chinnusamy V, Pareek A (2022) Photosynthesis: diving deep into the process in the era of climate change. *Plant Physiology Reports* 27: 539–542.
- Patra BC, Ray S, Ngangkham U, Mohapatra T (2016) Rice. In: *Genetic and Genomic Resources for Grain Cereals Improvement*. Singh M, Upadhyaya HD (eds). Academic Press, pp 1–80.
- Qu M, Hamdani S, Li W, Wang S, Tang J, Chen Z, Song Q, Li M, Zhao H, Chang T, Chu C, Zhu X (2016) Rapid stomatal response to fluctuating light: an under-explored mechanism to improve drought tolerance in rice. *Functional Plant Biology* 43(8): 727–738.
- Rantala M, Rantala S, Aro EM (2020) Composition, phosphorylation and dynamic organization of photosynthetic protein complexes in plant thylakoid membrane. *Photochemical & Photobiological Sciences* 19(5): 604–619.
- Sayre T, Negi S, Govindjee (2020) Light regulation of photosynthetic light harvesting doubles the biomass yield in the green alga *Chlamydomonas*. *Photosynthetica* 58(4): 974–975.
- Schauberger B, Archontoulis S, Arneth A, Balkovic J, Ciaia P, Deryng D, Elliot J, Folberth C, Khabarov N, Muller C, Pugh TA, Rolinski S, Schaphoff S, Schmid E, Wang X, Schlenker W, Frieler K (2017) Consistent negative response of US crops to high temperatures in observations and crop models. *Nature Communications* 8: 13931.

- Šetlík I, Allakhverdiev SI, Nedbal L, Šetlíková E, Klimov VV (1990) Three types of Photosystem II photoinactivation: I. Damaging processes on the acceptor side. *Photosynthesis Research* 23(1): 39–48.
- Shu S, Tang Y, Yuan Y, Sun J, Zhong M, Guo S (2016) The role of 24-epibrassinolide in the regulation of photosynthetic characteristics and nitrogen metabolism of tomato seedlings under a combined low temperature and weak light stress. *Plant Physiology and Biochemistry* 107: 344–353.
- Silva EN, Ferreira-Silva SL, Fontenele ADV, Ribeiro RV, Viégas RA, Silveira JAG (2010) Photosynthetic changes and protective mechanisms against oxidative damage subjected to isolated and combined drought and heat stresses in *Jatropha curcas* plants. *Journal of Plant Physiology* 167(14): 1157–1164.
- Soda N, Gupta BK, Anwar K, Sharan A, Govindjee, Singla-Pareek SL, Pareek A (2018) Rice intermediate filament, OsIF, stabilizes photosynthetic machinery and yield under salinity and heat stress. *Scientific Reports* 8(1): 4072.
- Stirbet A, Govindjee (2011) On the relation between the Kautsky effect (chlorophyll *a* fluorescence induction) and Photosystem II: Basics and applications of the OJIP fluorescence transient. *Journal of Photochemistry and Photobiology Biology* 104(1–2): 236–257.
- Stirbet A, Lazar D, Kromdijk J, Govindjee (2018) Chlorophyll *a* fluorescence induction: Can just a one-second measurement be used to quantify abiotic stress responses? *Photosynthetica* 56(1): 86–104.
- Strasser BJ, Strasser RJ (1995) Measuring Fast Fluorescence Transients to Address Environmental Questions: The JIP-test. In: Mathis P (ed.), *Photosynthesis: From Light to Biosphere*, Kluwer Academic Publishers, Dordrecht, pp 977–980.
- Strasser RJ, Srivastava A, Govindjee (1995) Polyphasic chlorophyll *a* fluorescence transient in plants and cyanobacteria. *Photochemistry and Photobiology* 61(1): 32–42.
- Strasser RJ, Tsimilli-Michael M, Srivastava A. (2004) Analysis of the chlorophyll *a* fluorescence transient. In: Papageorgiou GC, Govindjee (Eds.), *Chlorophyll *a* Fluorescence: A Signature of Photosynthesis. Advances in Photosynthesis and Respiration Series*, Dordrecht: Kluwer Academic Publishers, pp. 321–362.
- Suzuki N, Rivero RM, Shulaev V, Blumwald E, Mittler R (2014) Abiotic and biotic stress combinations. *New Phytologist* 203(1): 32–43.
- Tilman D, Balzer C, Hill J, Belfort BL (2011) Global food demand and the sustainable intensification of agriculture. *Proceedings of the National Academy of Sciences*, 108(50): 20260–4.
- Tsimilli-Michael M (2019) Revisiting JIP-test: An educative review on concepts, assumptions, approximations, definitions and terminology. *Photosynthetica* 57(S1): 90–107.
- Wungrampha S, Joshi R, Rathore RS, Singla-Pareek SL, Govindjee, Pareek A (2019) CO₂ uptake and chlorophyll *a* fluorescence of *Suaeda frutescens* grown under diurnal rhythm and after transfer to continuous dark. *Photosynthesis Research* 142(2): 211–227.
- Yadav C, Bahuguna RN, Dhankher OP, Singla-Pareek SL, Pareek A (2022) Physiological and molecular signatures reveal differential response of rice genotypes to drought and drought combination with heat and salinity stress. *Physiology and Molecular Biology of Plants* 28(4): 899–910.
- Yamori W, von-Caemmerer S (2009) Effect of Rubisco Activase Deficiency on the Temperature Response of CO₂ Assimilation Rate and Rubisco Activation State: Insights from Transgenic Tobacco with Reduced Amounts of Rubisco Activase. *Plant Physiology* 151(4): 2073–82.
- Yeung E, van Veen H, Vashisht D, Paiva ALS, Hummel M, Rankenberg T, Steffens B, Steffen-Heins A, Sauter M, de Vries M, Schuurink RC, Bazin J, Bailey-Serres J, Voesenek LACJ, Sasidharan R (2018) A stress recovery signaling network for enhanced flooding tolerance in *Arabidopsis thaliana*. *Proceedings of the National Academy of Sciences* 115(26): E6085–E6094.
- Zhang H, Mittal N, Leamy LJ, Barazani O, Song BH (2017) Back into the wild: Apply untapped genetic diversity of wild relatives for crop improvement. *Evolutionary Applications* 10(1): 5–24.

SUPPORTING INFORMATION

Additional supporting information can be found online in the Supporting Information section at the end of this article.

How to cite this article: Anwar, K., Joshi, R., Bahuguna, R.N., Govindjee, G., Sasidharan, R., Singla-Pareek, S.L. et al. (2024) Impact of individual, combined and sequential stress on photosynthesis machinery in rice (*Oryza sativa* L). *Physiologia Plantarum*, 176(1), e14209. Available from: <https://doi.org/10.1111/ppl.14209>